Fluorescent Micelles

Deutsche Ausgabe: DOI: 10.1002/ange.201507236
Internationale Ausgabe: DOI: 10.1002/anie.201507236

Synthesis and Design of Aggregation-Induced Emission Surfactants: Direct Observation of Micelle Transitions and Microemulsion Droplets

Weijiang Guan, Wenjuan Zhou, Chao Lu, and Ben Zhong Tang**

Abstract: *The direct visualization of micelle transitions is a long-standing challenge owing to the intractable aggregation-caused quenching of light emission in the micelle solution. Herein, we report the synthesis of a surfactant with a tetraphenylethene (TPE) core and aggregation-induced emission (AIE) characteristics. The transition processes of surfactant micelles and the microemulsion droplets (MEDs) formed by the surfactant with a TPE core were clearly visualized by a high-contrast fluorescence imaging method. The fluorescence intensity of the MEDs decreased as the size of MEDs increased as a result of weakening of the restriction of intramolecular rotation (RIR). The results of this study deepen our understanding of micelle-transition processes and provide solid evidence in favor of the hypothesis that the AIE phenomenon has its origin in the RIR of fluorophores in the aggregate state.*

Surfactants have been widely used in many areas, from basic technologies in daily products to advanced applications in biotechnology and nanomedicine.[1] Although an ancient subject, transition processes of surfactant micelles are still a topic of intense interest in both academic and technological research.[2] Kinetic monitoring of transition processes of micelles from spherical to wormlike micelles by in situ small-angle X-ray scattering (SAXS) has led to an impressive amount of data.[3] The development of a visualization technology would open new opportunities for the interrogation of the world of micelles. However, the direct visualization of micelle transitions by a high-contrast fluorescence imaging method has not yet been described.

A micelle is an aggregation of surfactant unimers in aqueous solution as a result of the inevitable process of surfactant self-assembly when the concentration of the surfactant is greater than the critical micelle concentration (CMC).[4] In principle, the formation of micelles could be directly visualized by confocal fluorescence microscopy (CFM) if the micellar aggregates could emit light. Although the unimers of well-known fluorescent surfactants emit intensely, their luminescence is quenched upon the formation of micelles as a result of the intrinsic aggregation-caused-quenching (ACQ) effect.[5] Therefore, the direct visualization of micelle transitions seems to be a great challenge.

An important class of aggregation-induced emission (AIE) materials have emerged: molecules that are non-emissive in the solution state but are induced to emit intensely upon aggregate formation.[6] Since then, a large number of new AIE-active materials, in which tetraphenylethene (TPE) is a typical structural unit, have been explored for their potential application in a wide range of fields, such as optical sensing, bioimaging, and optoelectronic devices.[7] Therefore, it is reasonable to anticipate that the direct visualization of surfactant-micelle-transition processes may be enabled by the design of TPE-based surfactants, thus avoiding the widespread occurrence of ACQ in micelles of conventional fluorescent surfactants.

In this study, we incorporated TPE units into sodium dodecyl sulfonate (SDS) molecules to generate luminescent surfactant (denoted as TPE-SDS) with AIE characteristics. Fluorescence microscopy was used for the direct visualization of the as-prepared TPE-SDS micelles in aqueous solution with excellent imaging contrast. More interestingly, the micellar transition that occurred during the continuous addition of a salt could also be visualized directly. We found that the original spherical micelles are first fused into bigger rodlike micelles, and that these rods continue to grow into wormlike micelles. Furthermore, the microemulsion droplets (MEDs) formed from TPE-SDS could also be observed directly, and the fluorescence intensity of MEDs was found to be inversely proportional to their size, because the restriction of intramolecular rotation (RIR) of TPE units is gradually weakened.

The synthetic route to the amphipathic TPE-SDS surfactant is outlined in Figure 1 A. The fluorescent TPE-2OH core (**1**) was prepared readily through McMurry coupling of 4-hydroxybenzophenone.[8] Its molecular structure was verified by ^{1}H NMR spectroscopy (see Figure S1 in the Supporting Information). TPE-2OH was treated with NaH (1 equiv) to activate one of the two hydroxy groups for the installation of a hydrophobic tail ($-(CH_2)_7CH_3$) to provide **2**. The structure of compound **2** was confirmed by ^{1}H NMR spectroscopy, ^{13}C NMR spectroscopy, and mass spectrometry (see Figures S2–S4). It was necessary to purify compound **2** by silica-gel column chromatography to assure the complete removal of unreacted TPE-2OH. Next, compound **2** was transformed

[*] Dr. W. Guan, Dr. W. Zhou, Prof. Dr. C. Lu
State Key Laboratory of Chemical Resource Engineering
Beijing University of Chemical Technology
P.O. Box 79, 100029, Beijing (China)
E-mail: luchao@mail.buct.edu.cn
Prof. Dr. B. Z. Tang
Department of Chemistry
The Hong Kong University of Science and Technology
Clear Water Bay, Kowloon, Hong Kong (China)
E-mail: tangbenz@ust.hk

Supporting information for this article is available on the WWW under http://dx.doi.org/10.1002/anie.201507236.

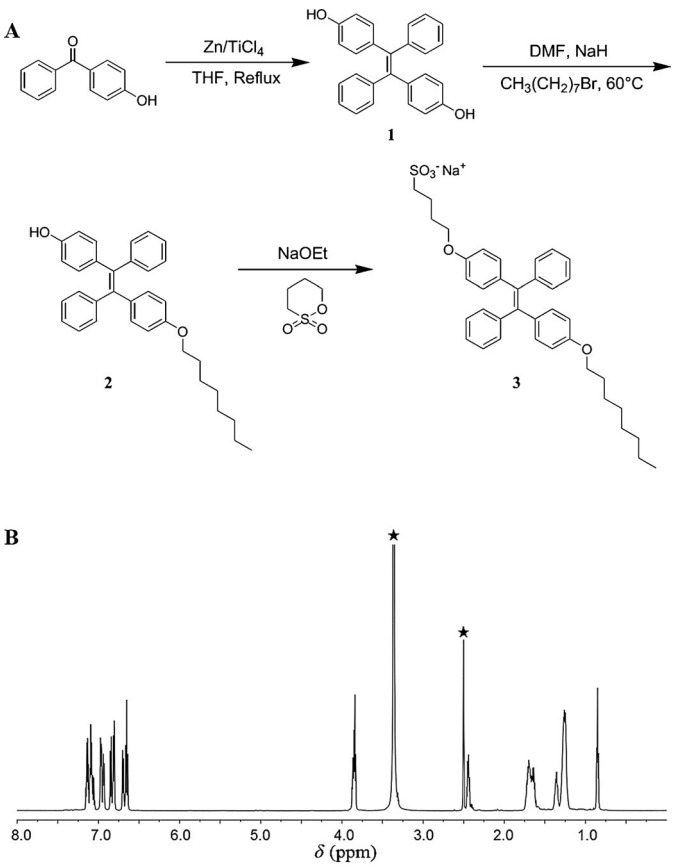

Figure 1. A) Synthetic route to the amphipathic surfactant TPE-SDS (**3**). B) ^{1}H NMR spectrum of TPE-SDS in [D_6]dimethyl sulfoxide (the solvent peaks are marked with asterisks). C) Negative-ion ESIMS spectrum of TPE-SDS. DMF = *N*,*N*-dimethylformamide.

into a sodium salt in a basic environment and treated with 1,4-butanesultone to introduce a sulfonate substituent ($-(CH_2)_4SO_3^-$). The structure of the product TPE-SDS (**3**) was confirmed by the presence of resonance peaks in the ^{1}H NMR spectrum for all alkyl hydrogen atoms (Figure 1B). A mass-to-charge (m/z) ratio of 611.2842 in the MS spectrum further proved the formation of TPE-SDS (Figure 1C). This value is consistent with the exact mass generated for this compound by the software ChemDraw Ultra 12.0. The structure of TPE-SDSA was also verified by ^{13}C NMR spectroscopy (see Figure S5).

The surface activity of the as-prepared surfactant TPE-SDS in aqueous solution was evaluated through the measurement of surface tension.[9] A plot of surface tension (γ) versus TPE-SDS concentration (log(C); Figure 2A) shows

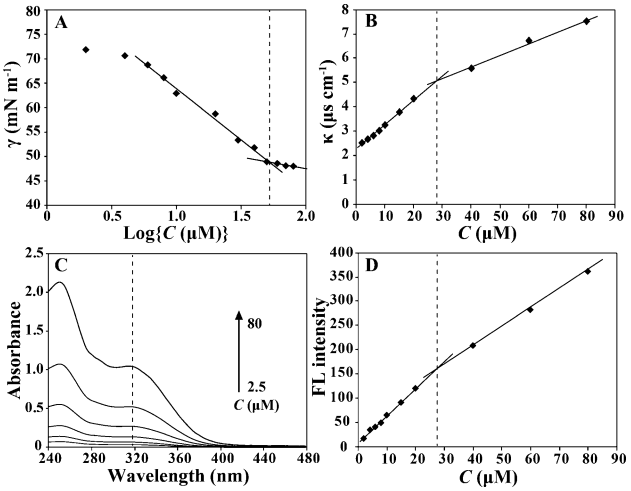

Figure 2. A) Plot of surface tension versus log(concentration) for TPE-SDS. B) Plot of conductivity versus the concentration of TPE-SDS. C) Absorption spectra of TPE-SDS at different concentrations. D) Plot of fluorescence intensity at 490 nm versus the corresponding TPE-SDS concentration.

that at low concentrations, the TPE-SDS unimers were preferentially adsorbed at the air–water interface, thus leading to a sharp reduction in the surface tension of water. When the concentration of TPE-SDS continued to increase, the adsorption of TPE-SDS at the air–water interface reached a saturation state, and thus a relatively constant surface tension was observed. An inflection point appears at around 50 μM, indicative of the CMC of the surfactant TPE-SDS.

The CMC value of TPE-SDS could be measured readily by the method of conductivity variation.[10] The conductivity (κ) of TPE-SDS in water is plotted against its concentration (C) in Figure 2B. The conductivity increased linearly as the concentration of TPE-SDS increased up to 30 μM; however, when the concentration was higher than 30 μM, the plot was linear with a lower slope, thus indicating an increase in the mass-per-unit charge of TPE-SDS. This break between the two slopes indicates the formation of TPE-SDS micelles.[1b] These results, along with those obtained by surface-tension measurements, strongly demonstrated that the as-prepared TPE-SDS was a typical anionic surfactant. Furthermore, a transmission electron microscopy (TEM) image of 40 μM TPE-SDS showed a spherical structure of the TPE-SDS micelles with a radius of (3.5 ± 0.5) nm (see Figure S6A), which is almost equal to the extended length of a TPE-SDS molecule (i.e., 2.97 nm).

The optical properties of the surfactant TPE-SDS were studied by UV/Vis absorption and fluorescence spectroscopy. The absorption spectra (Figure 2C) showed two peaks, at 250 and 318 nm. They were assigned to the absorption of the phenyl groups and the conjugated TPE, respectively.[11] Their

intensity increased linearly with the TPE-SDS concentration in the range from 2.5 to 80 μM. The peak position at 318 nm remained unchanged as the TPE-SDS concentration increased; in contrast, a clear peak shift occurred for reported aggregates of TPE derivatives.[12] This difference between TPE-SDS and other AIE molecules with a TPE core indicated that the conformation of the TPE-SDS molecules did not depend on the micelle aggregates.

In general, the luminescence of AIE molecules is triggered by aggregate formation.[13] Herein, the fluorescence excitation and emission spectra of TPE-SDS in aqueous solutions were studied (see Figure S7). The fluorescence intensity at 490 nm versus the corresponding TPE-SDS concentration is plotted in Figure 2D. The fluorescence of the surfactant TPE-SDS gradually increased as the TPE-SDS concentration increased. One inflection point appeared at around 30 μM (equal to the CMC obtained from conventional electrical conductivity method), thus suggesting a change in the aggregation state from surfactant unimers to micelles.[14] The decrease in the slope after the inflection point is possibly due to the increased freedom of the TPE units in the nonpolar interior of the micelles as compared to the aqueous environment.[1b]

The structure transition of the TPE-SDS micelles in the solution state was directly visualized by CFM. Fluorescence microscopy images of the TPE-SDS micelles in pure water, 0.5 M aqueous NaCl, and 1.0 M aqueous NaCl were taken with a 405 nm laser. Although the micelle size was outside the resolution of the CFM measurements, diffraction blur enabled the observation of the luminescent dots of the TPE-SDS micelles (Figure 3A,D). The spherical structure of the TPE-SDS micelles was further confirmed by TEM (see Figure S6A). The formation of the spherical structure was attributed to the strong electrostatic repulsion between the anionic head groups, thus leading to a high curvature of the TPE-SDS micelle core.[4] Furthermore, the electrical double layer formed at the micelle–water interface has a ζ-potential value of greater than −50 mV, thus demonstrating good dispersion stability of the resulting TPE-SDS micelles.

Generally, the effective thickness of the electrical double layer can be decreased in a controlled manner by the addition of neutral electrolytes (e.g., NaCl).[15] Rodlike micelles were directly observed when 0.5 M aqueous NaCl was added to the solution of the TPE-SDS micelles (Figure 3B,E) because the repulsion between anionic heads in the micelle is reduced when the electrical double layer surrounding the anionic heads is compressed.[4] Closer packing of the anionic heads leads to a transformation of micelle structure from spherical to rodlike. More interestingly, as the NaCl concentration was increased to 1.0 M, the tendency of the micelles to become elongated became more obvious until wormlike micelles could be clearly seen (Figure 3C,F). In conclusion, direct visualization clearly disclosed the processes of micelle transition from spherical, to rodlike, and finally to wormlike structures.

The micelle-transition processes were also investigated by other techniques, such as dynamic light scattering (DLS), TEM, and rheology measurements. TEM showed that the size of the micelles increased during the transition from spherical

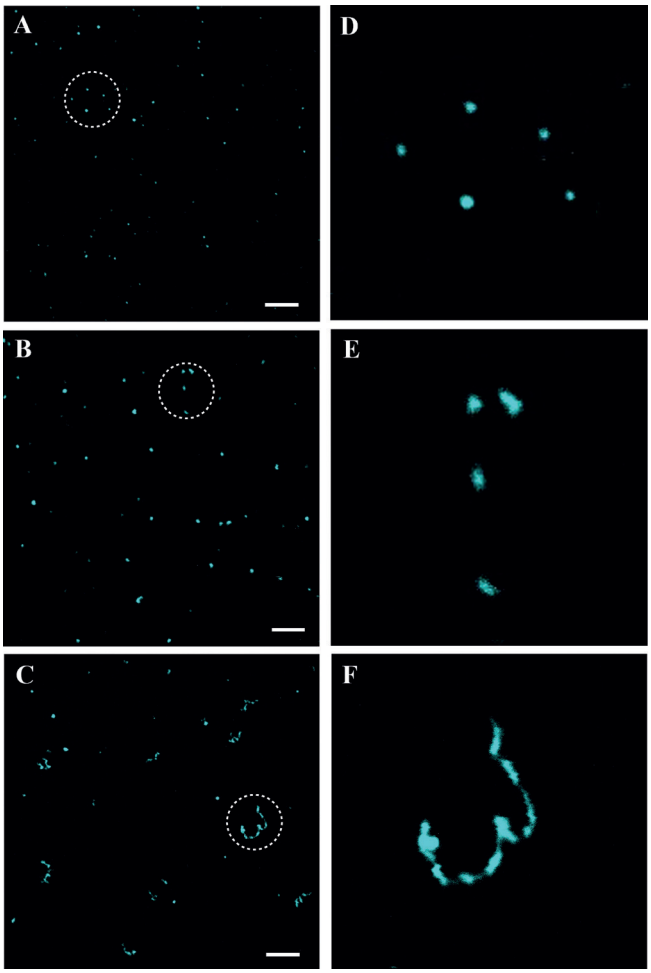

Figure 3. Fluorescence microscopy images of the TPE-SDS micelles in A) pure water, B) 0.5 M NaCl solution, and C) 1.0 M NaCl solution. D–F) Magnification of the indicated regions in (A–C). TPE-SDS concentration: 80 μM. Scale bars: 5 μm. All images were taken with a 405 nm laser.

to rodlike and finally wormlike micelles (see Figure S6). DLS measurements indicated that the average diameters of the spherical, rodlike, and wormlike micelles were 7.62, 214.2, and 2991 nm, respectively (see Figure S8). Rheology measurements provided additional information about the micelle transitions. We measured the zero-shear viscosity (η_0) of 80 μM solutions of TPE-SDS as a function of the NaCl concentration and found that at a low salt content (< 0.5 M), the viscosity increased slowly as the NaCl concentration increased, thus indicating the formation of rodlike micelles. When the concentration of NaCl continued to increase above 0.5 M, the rodlike micelles grew continuously longer to form wormlike micelles, thus resulting in a sharp increase in viscosity (see Figure S9).[16] In conclusion, the processes of micelle transition as determined by these measurement techniques were in good agreement with those found by CFM.

Although the origins of the AIE phenomenon are still under debate, the most widely accepted explanation involves the RIR of fluorophores in the aggregate state.[17] However, there is currently no solid evidence to support the claim. In

this study, we synthesized a water-in-oil (W/O) microemulsion system containing TPE-SDS, 1-butanol, isooctane, and water to measure the shortest distance between TPE units for the emission of light. Interestingly, we found that the fluorescence intensity decreased as the size of the MEDs increased (Figure 4A). The spherical structure of the formed MEDs was confirmed by CFM (Figure 4B).

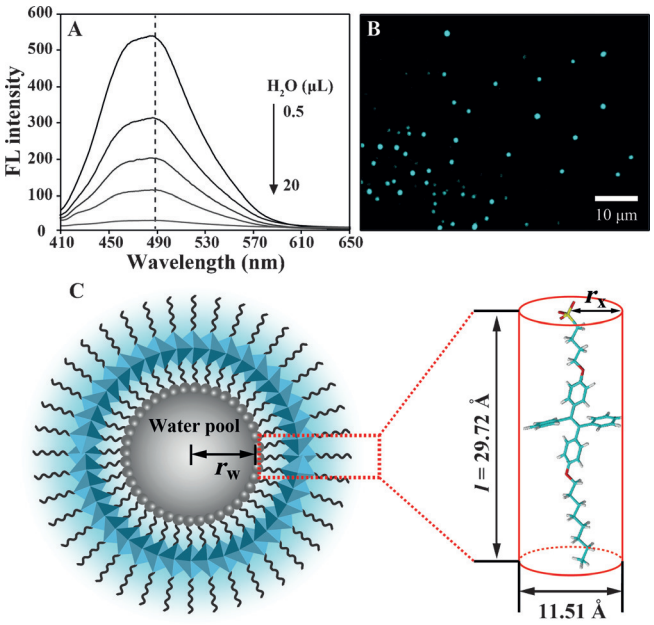

Figure 4. A) Fluorescence spectra of microemulsion solutions with differing water content (0.5, 5, 10, 15, and 20 μL; TPE-SDS: 2.0 nmol, isooctane volume: 3.2 mL, 1-butanol volume: 0.8 mL). B) Fluorescence microscopy image of a TPE-SDS microemulsion. C) Schematic illustration of a microemulsion droplet, and the TPE-SDS molecular model generated with the ACD Labs software.

We calculated the structural parameters of the W/O microemulsion by using a mathematical model (Figure 4C).[18] The TPE-SDS and 1-butanol molecules are arranged closely in an orderly fashion around the water pools so that the water pools are separated from the oil phase. In this model, we assume that the size of spherical MEDs is uniform. A TPE-SDS molecule is considered as a cylinder: The height of the cylinder is equal to the length of TPE-SDS (l), and the radius of the circle (r_x) is equal to half the estimated distance between two adjacent TPE units. The water-pool radius (r_w) is calculated by subtracting the TPE-SDS length (l) from the MED radius (r). The size of the MED was measured with a ζ-potential analyzer. The spheroidal volume of the MED (V) and the water pool (V_w) is given by Equations (1) and (2), respectively:

$$V = 4/3\,\pi r^3 \tag{1}$$

$$V_w = 4/3\,\pi r_w^3 = 4/3\,\pi (r-l)^3 \tag{2}$$

The number of water pools (N_w) in the microemulsion system is then obtained from Equation (3):

$$N_w = V_{w,t}/V_w \tag{3}$$

in which $V_{w,t}$ is the total volume of water in the microemulsion system. The average aggregation number of TPE-SDS molecules associated with a water pool is calculated by Equation (4):

$$N_s = n_s N_A/N_w \tag{4}$$

in which n_s and N_A are the total number of moles of TPE-SDS and the Avogadro constant, respectively. The effective volume (V_s) of a single TPE-SDS molecule as a cylinder can be written as:

$$V_s = \pi r_x^2 l \tag{5}$$

The volume of a single MED is equal to the sum of the volume of the TPE-SDS layer and the water pool:

$$V = V_w + N_s V_s \tag{6}$$

The value of r_x can be calculated by combining the above equations. We estimated the corresponding distance between two adjacent TPE units attached at water pools with different sizes. (Note that the amount of TPE-SDS used to synthesize the microemulsion system was 2.0 nmol.) For example, if 0.5 μL of water is added, the radius of the water pool is calculated to be 11.76 nm. The estimated distance between two adjacent TPE units is 0.54 nm, which is equal to half the TPE length. In this case, the TPE units could be effectively restricted so that the formed microemulsion could emit intense light. If 20 μL of water is added, the fluorescence intensity of the microemulsion is close to zero, possibly because the rotation of the two free phenyl groups on the TPE core can not be effectively restricted. In this case, the radius of the water pool is increased to 66.00 nm, with a distance of 1.10 nm between two adjacent TPE units. Therefore, we conclude that MEDs cannot be directly visualized by CFM if the distance between two adjacent TPE units is above 1.10 nm.

In conclusion, we have presented the synthesis and micelle characteristics of a novel kind of anionic surfactant, TPE-SDS, with an AIE effect. Micelle-transition processes (involving spherical micelles, rodlike micelles, and wormlike micelles) and TPE-SDS MEDs were directly visualized by CFM. In comparison to other currently available techniques, the high-resolution imaging method offers a clear view into the world of micelles. Furthermore, the fluorescence intensity of MEDs indicated their size. This study not only establishes a feasible method for the imaging of micelle-transition processes, but also deepens our understanding of the AIE effect. This facile method may open viable opportunities and inspiration for the direct visualization of other self-assembly processes of materials related to surfactants. The results of our current efforts toward these objectives will be reported in due course.

Acknowledgements

This research was supported by the National Basic Research Program of China (973 Program, 2014CB932103), the National Natural Science Foundation of China (21375006 and 21575010), and the Innovation and Promotion Project of Beijing University of Chemical Technology.

Keywords: aggregation-induced emission · fluorescence · micelles · microemulsions · surfactants

How to cite: *Angew. Chem. Int. Ed.* **2015**, *54*, 15160–15164
Angew. Chem. **2015**, *127*, 15375–15379

[1] a) D. Hu, K. C. Chou, *J. Am. Chem. Soc.* **2014**, *136*, 15114–15117; b) M. J. Rosen, J. T. Kunjappu, *Surfactants and Interfacial Phenomena*, Wiley, Hoboken, NJ, **2012**; c) K. Holmberg, B. Jönsson, B. Kronberg, B. Lindman, *Surfactants and Polymers in Aqueous Solution*, Wiley, Chichester, **2002**; d) E. Soussan, S. Cassel, M. Blanzat, I. Rico-Lattes, *Angew. Chem. Int. Ed.* **2009**, *48*, 274–288; *Angew. Chem.* **2009**, *121*, 280–295.

[2] a) H. Hoffmann, G. Ebert, *Angew. Chem. Int. Ed. Engl.* **1988**, *27*, 902–912; *Angew. Chem.* **1988**, *100*, 933–944; b) S. Ezrahi, E. Tuval, A. Aserin, *Adv. Colloid Interface Sci.* **2006**, *128–130*, 77–102; c) G. V. Jensen, R. Lund, J. Gummel, M. Monkenbusch, T. Narayanan, J. S. Pedersen, *J. Am. Chem. Soc.* **2013**, *135*, 7214–7222.

[3] G. V. Jensen, R. Lund, J. Gummel, T. Narayanan, J. S. Pedersen, *Angew. Chem. Int. Ed.* **2014**, *53*, 11524–11528; *Angew. Chem.* **2014**, *126*, 11708–11712.

[4] B. Kronberg, K. Holmberg, B. Lindman, *Surface Chemistry of Surfactants and Polymers*, Wiley, Chichester, **2014**.

[5] a) F.-Y. Tsai, H.-L. Tu, C.-Y. Mou, *J. Mater. Chem.* **2006**, *16*, 348–350; b) M. Štěpánek, K. Procházka, *Langmuir* **1999**, *15*, 8800–8806.

[6] J. D. Luo, Z. L. Xie, J. W. Y. Lam, L. Cheng, H. Y. Chen, C. F. Qiu, H. S. Kwok, X. W. Zhan, Y. Q. Liu, D. B. Zhu, B. Z. Tang, *Chem. Commun.* **2001**, 1740–1741.

[7] a) Y. N. Hong, J. W. Y. Lam, B. Z. Tang, *Chem. Soc. Rev.* **2011**, *40*, 5361–5388; b) D. Ding, K. Li, B. Liu, B. Z. Tang, *Acc. Chem. Res.* **2013**, *46*, 2441–2453; c) R. R. Hu, N. L. C. Leung, B. Z. Tang, *Chem. Soc. Rev.* **2014**, *43*, 4494–4562; d) J. Mei, Y. N. Hong, J. W. Y. Lam, A. J. Qin, Y. H. Tang, B. Z. Tang, *Adv. Mater.* **2014**, *26*, 5429–5479.

[8] C. M. Yu, Y. L. Wu, F. Zeng, X. Z. Li, J. B. Shi, S. Z. Wu, *Biomacromolecules* **2013**, *14*, 4507–4514.

[9] P. C. Yin, P. F. Wu, Z. C. Xiao, D. Li, E. Bitterlich, J. Zhang, P. Cheng, D. V. Vezenov, T. B. Liu, Y. G. Wei, *Angew. Chem. Int. Ed.* **2011**, *50*, 2521–2525; *Angew. Chem.* **2011**, *123*, 2569–2573.

[10] L. Shi, D. Lundberg, D. G. Musaev, F. M. Menger, *Angew. Chem. Int. Ed.* **2007**, *46*, 5889–5891; *Angew. Chem.* **2007**, *119*, 5993–5995.

[11] H. Tong, Y. N. Hong, Y. Q. Dong, M. Häussler, Z. Li, J. W. Y. Lam, Y. P. Dong, H. H.-Y. Sung, I. D. Williams, B. Z. Tang, *J. Phys. Chem. B* **2007**, *111*, 11817–11823.

[12] a) S.-B. Han, H.-J. Kim, D. Jung, J. Kim, B.-K. Cho, S. Cho, *J. Phys. Chem. C* **2015**, *119*, 16223–16229; b) A. Rananaware, R. S. Bhosale, K. Ohkubo, H. Patil, L. A. Jones, S. L. Jackson, S. Fukuzumi, S. V. Bhosale, S. V. Bhosale, *J. Org. Chem.* **2015**, *80*, 3832–3840; c) J. Wang, J. Mei, R. R. Hu, J. Z. Sun, A. J. Qin, B. Z. Tang, *J. Am. Chem. Soc.* **2012**, *134*, 9956–9966.

[13] a) J. W. Li, Y. Li, C. Y. K. Chan, R. T. K. Kwok, H. K. Li, P. Zrazhevskiy, X. H. Gao, J. Z. Sun, A. J. Qin, B. Z. Tang, *Angew. Chem. Int. Ed.* **2014**, *53*, 13518–13522; *Angew. Chem.* **2014**, *126*, 13736–13740; b) Y. Okazawa, K. Kondo, M. Akita, M. Yoshizawa, *J. Am. Chem. Soc.* **2015**, *137*, 98–101.

[14] Y. J. Xia, L. Dong, Y. Z. Jin, S. Wang, L. Yan, S. C. Yin, S. X. Zhou, B. Song, *J. Mater. Chem. B* **2015**, *3*, 491–497.

[15] a) D. C. Grahame, *Chem. Rev.* **1947**, *41*, 441–501; b) J. J. López-García, J. Horno, C. Grosse, *Langmuir* **2011**, *27*, 13970–13974.

[16] a) J.-H. Mu, G.-Z. Li, X.-L. Jia, H.-X. Wang, G.-Y. Zhang, *J. Phys. Chem. B* **2002**, *106*, 11685–11693; b) P. A. Hassan, S. R. Raghavan, E. W. Kaler, *Langmuir* **2002**, *18*, 2543–2548.

[17] a) N. B. Shustova, B. D. McCarthy, M. Dincă, *J. Am. Chem. Soc.* **2011**, *133*, 20126–20129; b) N. B. Shustova, A. F. Cozzolino, V. K. Michaelis, R. G. Griffin, M. Dincă, *J. Am. Chem. Soc.* **2012**, *134*, 15061–15070; c) N. B. Shustova, A. F. Cozzolino, S. Reineke, M. Baldo, M. Dincă, *J. Am. Chem. Soc.* **2013**, *135*, 13326–13329; d) J. Zhao, D. Yang, Y. X. Zhao, X.-J. Yang, Y.-Y. Wang, B. Wu, *Angew. Chem. Int. Ed.* **2014**, *53*, 6632–6636; *Angew. Chem.* **2014**, *126*, 6750–6754.

[18] a) S. Bardhan, K. Kundu, G. Chakraborty, S. K. Saha, B. K. Paul, *J. Surfactants Deterg.* **2015**, *18*, 547–567; b) S. K. Hait, S. P. Moulik, *Langmuir* **2002**, *18*, 6736–6744.

Received: August 3, 2015
Revised: September 18, 2015
Published online: October 16, 2015

